

DOI: 10.1002/anie.202015625

# Covalent cell surface conjugation of nanoparticles by a combination of metabolic labelling and click chemistry

Alexander Lamoot, [a] Annemiek Uvyn, [a] Sabah Kasmi, [a] Bruno G. De Geest*[a]

[a] A Lamoot; A Uvyn, Dr. S Kasmi, Prof.Dr. BG De Geest.
Department of Pharmaceutics, Ghent University, Ghent, Belgium

Supporting information for this article is given via a link at the end of the document.

**Abstract:** Conjugation of nanoparticles (NP) to the surface of living cells is of interest in the context of exploiting the tissue homing properties of *ex* vivo engineered T cells for tumor targeted delivery of drugs loaded into NP. Cell surface conjugation requires either a covalent or non-covalent reaction. Non-covalent conjugation with ligand decorated NP is challenging and involves a dynamic equilibrium between the bound and unbound state. Covalent NP conjugation results in a permanently bound state of NP, but the current routes for cell surface conjugation face slow reaction kinetics and random conjugation to proteins in the glycocalyx. To address the unmet need for alternative bio-orthogonal strategies that allow for efficient covalent cell surface conjugation, we developed a 2-step click conjugation sequence in which cells are first metabolically labelled with azides followed by reaction with sulfo-6-methyl-*tetrazine*-dibenzyl cyclooctyne (Tz-DBCO) by SPAAC, and subsequent IEDDA with transcyclooctene (TCO) functionalized NP. In contrast to using only metabolic azide labelling and subsequent conjugation of DBCO-NP, our 2-step yields a highly specific cell surface conjugation of LNP, with very low non-specific background binding.

## Introduction

Conjugating nanoparticles (NP) to the surface of live cells is an attractive strategy to exploit the tissue-homing properties of specific cell types for targeted delivery of drugs loaded into these NP.[1] Therapeutic examples are *ex vivo* engineering of tumor-infiltrating T lymphocytes and CAR T cells [2] to carry with high specificity pharmacologically active compounds into the tumor microenvironment. Two major routes of cell surface conjugation involve either covalent [3] or non-covalent (bio)chemical reaction [4]. Non-covalent conjugation typically relies on ligand-decorated NP that subsequently bind to a cell surface receptor. Whereas this approach is conceptually sound, the reality is more daunting as in most cases, suitable ligands are antibodies or antibody fragments, which pose particular challenges with regard to site-specific conjugation and orientation [5] to achieve high affinity receptor binding. Moreover, protein-based ligand-decorated NP involve major challenges with regard to controlled and reproducible assembly as well as QA. Taking into account the high cost of recombinant protein synthesis, it might be not surprising that currently no protein-based ligand-decorated NP are on the market. Covalent conjugation makes use of reactive groups in the cellular glycocalyx to form a covalent bond with a complimentary reaction partner on the NP surface. In this context, mostly lysines and cysteines are targeted using respectively activated esters and maleimides.[3] Also these routes face important drawbacks: (a) Conjugation occurs randomly to proteins of the glycocalyx, which can negatively affect the biological activity of these proteins. (b) Amide and thioether bond formation tend to be sluggish at low concentration and slow diffusion of the reaction partners, which is the case when conjugating large sterically hindered objects such as cells and NP. (c) Maleimides and particularly activate esters are unstable in aqueous medium and can conjugate randomly to proteins in the cell culture medium.[6][7] (d) For maleimide-based conjugation, an additional blocking step with a thiolated compound is required after conjugation to block unreacted maleimides and prevent these from unwanted protein binding later on.[8]

Hence, a clear need exists for simple strategies that allow for covalent cell surface conjugation of NP with good efficiency and selectivity. In this regard, bio-orthogonal click reactions are an attractive alternative.[9] Moreover, the ease by which azides can be introduced onto a cell surface through metabolic labelling with azido sugars allows for introducing a high density of synthetic low molecular weight cell surface receptors with a reported minimal influence on the cellular functionality.[10][11][12] Azides immediately prompt the combination with strained cycloalkynes as complimentary reaction partners to form a stable triazole bond through the efficient and highly bio-orthogonal strain-promoted azide-alkyne cycloaddition (SPAAC) reaction.[10] This was the starting point of the present paper where we aimed to investigate bio-orthogonal routes for cell surface conjugation of NP. **Scheme 1** schematically illustrates these strategies.

**Scheme 1** | Overview of the strategies elaborated in this work for of bio-orthogonal for cell surface conjugation. (A->B) Cells are metabolically labelled by addition of Ac4ManN3 to the culture medium, installing azides within the glycocalyx. (B->C) Metabolically azide labelled cells can be conjugated with cyclooctyne-functionalized NP by SPAAC. (B->B*->C) To increase the conjugation efficiency and intermediate pH-switch can be applied. At pH 5, NP containing an ionizable lipid with pKa between 6 and 8, bear a positive charge, leading to adsorption of NP to the negatively charged phospholipid cell membrane by electrostatic interaction, followed by SPAAC conjugation of NP to cell surface azides. (B->D) Cell surface azides are conjugated with a low molecular weight cyclooctyne-tetrazine compound followed by (D->E) conjugation of cyclooctene-functionalized NP by IEDDA.

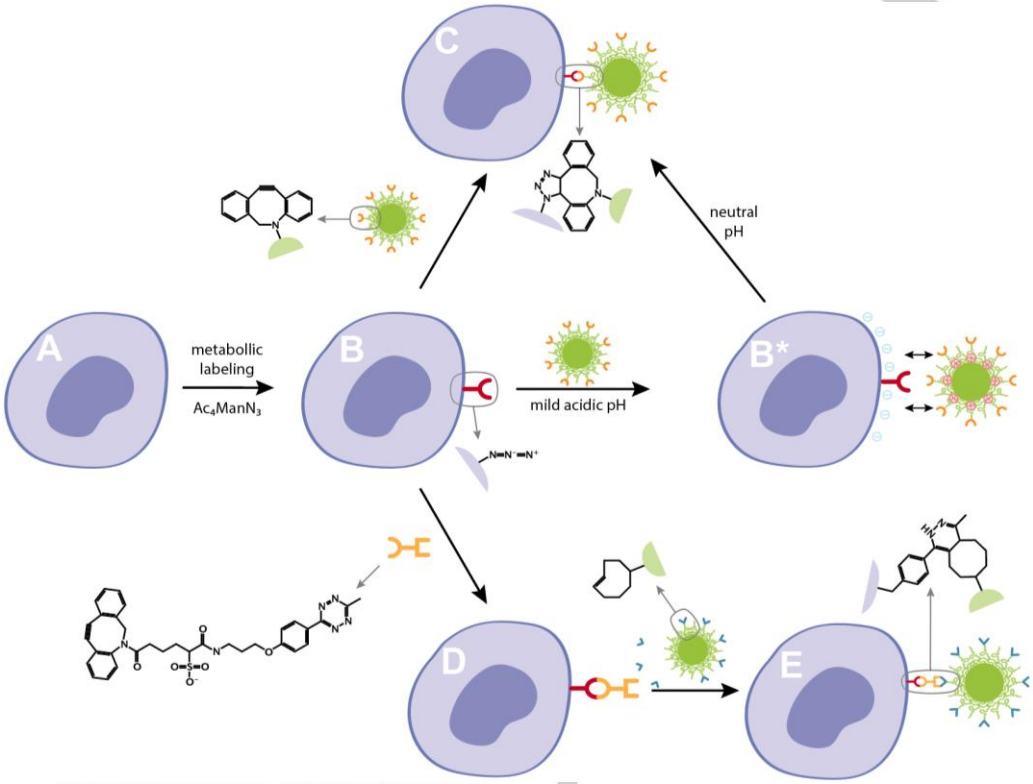


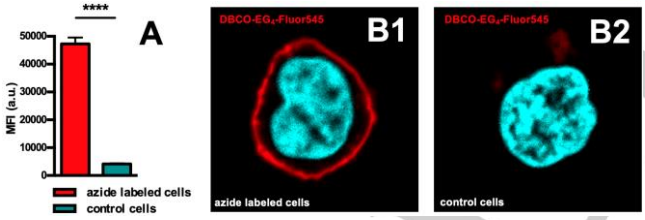


**Figure 1** | Flow cytometry analysis (n=3; t-test **** p<0,0001) (A) and confocal microscopy (B) of metabolic labelled cells and control cells incubated with DBCO-EG4-Fluor545 (red fluorescence). Cell nuclei were stained with Hoechst (cyan). Scale bar represents 5 micron.

## Results and Discussion

First, to set benchmark conditions, we verified whether, in our chosen experimental framework, cells can become successfully metabolically azide labelled and subsequently covalently conjugated by SPAAC with a dibenzocyclooctyne (DBCO)-functionalized fluorophore. Hereto, Jurkat T cells, a model immortalized human T cell line, were incubated for 48h with 25 μM of N-azidoacetylmannosamine-tetraacetylated ($Ac_4ManN_3$), followed by treatment for 1 h with a 10 μM solution of DBCO-$EG_4$-Fluor545. Flow cytometry analysis provided clear proof of successful metabolic labelling and SPAAC conjugation with low non-specific background staining of cells that were not metabolically azide labelled (**Figure 1A**). Confocal microscopy imaging revealed that DBCO-$EG_4$-Fluor545 conjugation predominantly yielded staining of the cell surface (**Figure 1B**). Taken together, these findings are fully in line with previous reports by us and others.[10][12][13]

Having confirmed that under the specified conditions, Jurkat T cells can be successfully metabolically labelled and SPAAC conjugated, we endeavored into exploring the possibility to conjugate NP to the cell surface. For this purpose, we selected lipid nanoparticles (LNP) formed by electrostatic complexation of an ionizable cationic lipid and polyinosinic:polycytidylic acid (polyIC). PolyIC is a synthetic analogue of double stranded RNA and a potent agonist of Toll-like receptor 3 (TLR3) and thereby provokes innate immune activation which is of interest to achieve within the tumor microenvironment and in sentinel lymph nodes.[14][15] Hence, we reasoned that polyIC, as would also be the case for other TLR agonists including CpG as TLR9 and single stranded RNA or imidazoquinolines as TLR7/8 agonists [16][17][18], would be well suited for T cell mediated tumor targeted

delivery. Owing to its macromolecular polyanionic nature, polyIC does not efficiently enters cells by endocytosis

**Table 1**| LNP characteristics: mean particle size, PDI and zeta potential measured in acetate buffer (5 mM) pH 5 and HEPES buffer (5 mM) pH 7.4 (mean ± SD)

| LNP formulation | Z-average (nm)± SD | PDI ± SD | Zeta potential (mV) ± SD | |
|---|---|---|---|---|
| | | | pH 5 | pH 7.4 |
| DSPE-PEG-DBCO (**DBCO LNP**) | 158 ± 0.5 | 0.26 ± 0.01 | 12 ± 4 | −19 ± 5 |
| DSG-PEG (control LNP) | 133 ± 1.2 | 0.15 ± 0.01 | 17 ± 6 | −8 ± 5 |
| DSPE-PEG-TCO 1.5% (**TCO LNP 1.5%**) | 142 ± 1.8 | 0.16 ± 0.02 | 21 ± 4 | −26 ± 5 |
| DSPE-PEG-TCO 1.0% (**TCO LNP 1.0%**) | 128 ± 0.3 | 0.16 ± 0.01 | 25 ± 3 | −13 ± 5 |
| DSPE-PEG-TCO 0.5% (**TCO LNP 0.5%**) | 96 ± 0.3 | 0.14 ± 0.01 | 25 ± 8 | −3 ± 5 |

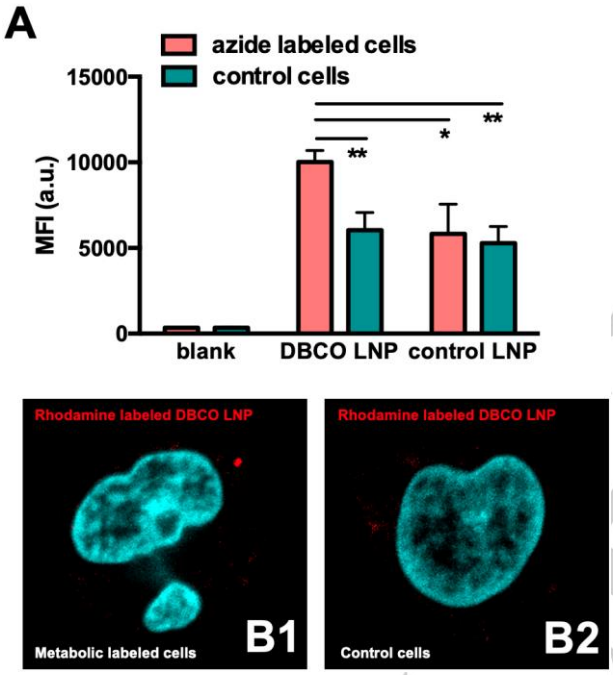


**Figure 2**| Flow cytometry analysis (n=3; t-test * p<0,05; ** p<0,01) (A) and confocal microscopy (B) of metabolic labelled cells (B1) and control cells incubated (B2) with DBCO LNP and control LNP. Cell nuclei were stained with Hoechst (cyan). Scale bar represents 5 micron.

due to electrostatic repulsion by the also anionic phospholipid cell membrane, and also faces degradation by nucleases.[15] Hence, formulation into a carrier that favours delivery into endosomal vesicles where TLR3 is located should be a viable strategy to improve the therapeutic activity of polyIC. In this context, we reasoned that LNP containing also helper lipids (i.e. cholesterol to aid in LNP stabilization) and PEGylated lipids (require for colloidal stabilization), a concept borrowed from the RNA delivery field [19],would be well suited to promote uptake by innate immune cells such as dendritic cells (DCs) and macrophages once release from the T cell surface in the tumor microenvironment.

LNP encapsulating polyIC were prepared by solvent displacement by mixing an ethanolic solution containing all lipids and an aqueous solution containing polyIC, followed by removal of the ethanol by dialysis. As PEGylated lipids we used 1,2-distearoyl-sn-glycero-3-phosphoethanolamine-N-(dibenzocyclooctyl(polyethylene glycol)) (DSPE-PEG-DBCO) and 1,2-distearoyl-rac-glycero-3-methylpolyethylene glycol (DSG-PEG), both with a PEG length of 2 kDa. LNP size and electrophoretic mobility were measured **(Table 1)**, thereby revealing similar characteristics for both LNPs, with a mean diameter of 145 nm and a negative zeta potential of -14 mV at physiological pH of 7.4 and a positive value of 15 mV at a pH of 5. The latter is due to the pKa of the isopropylamino group of the ionizable lipid and which has a pKa situated around 6 **(Figure S1)**. hence leading to a low extent of ionization at neutral pH and a high extent of ionization at acidic pH.

Subsequently we tested whether DBCO LNP can be selectively SPAAC-conjugated to metabolically azide labelled cells. Flow cytometry analysis showed a modest although significant increase in cellular fluorescence, relative to non-metabolically labelled control cells, and control LNP that did not contain DBCO. Presence of LNP on the cell surface was confirmed by confocal microscopy **(Figure 2)**. However, it was also clear that a significant background staining occurred by LNP that were associated to cells, irrespective of the presence of azides or DBCO on either cells or LNP. When attempting to increase the extent of LNP conjugation by prolonging the incubation time of cells and LNP **(Figure S2)**, we noticed that one could indeed increase the cellular fluorescence, but unfortunately, also the non-specific LNP background adsorption increased. A similar situation was encountered when e.g. increase the concentration of LNP.

Fostered by the pH-dependent degree of ionization of the cationic lipid in the LNP, with resulting positive zeta potential at pH 5, we reasoned that incubation of cells and LNP at such mild acidic pH, could potentially enhance the efficiency of DBCO LNP conjugation to azides in the cellular glycocalyx. By promoting electrostatic interaction between positively charged LNP and the negatively charged phospholipid cell membrane, one addresses the issue of the low local concentration of slowly diffusing

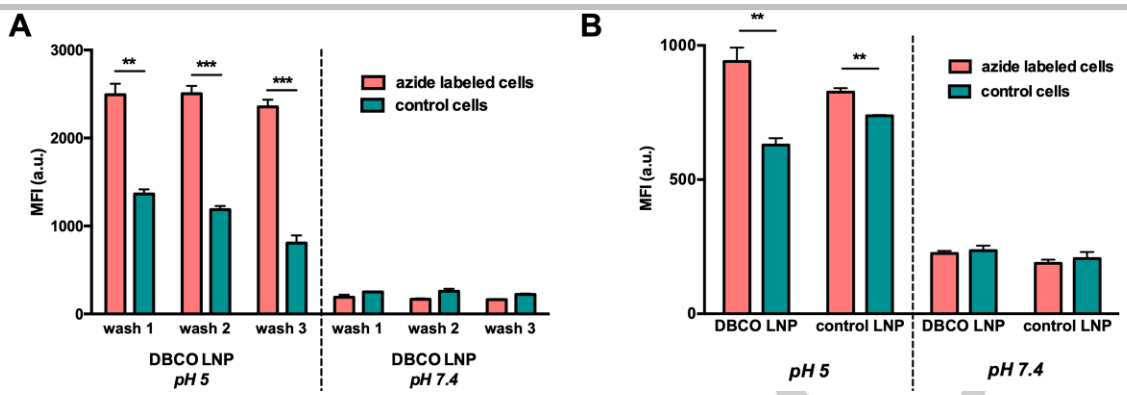


**Figure 3** | Flow cytometry analysis of metabolic labelled cells and control cells incubated 15 min (A) with DBCO LNP at pH 5 or pH 7.4 and washed thrice with pH 7.4, (B) with DBCO LNP and control LNP at pH5 or pH 7.4 and washed thrice with pH 7.4. (n=3; t-test ** p<0,01; *** p<0,001)

reaction partners. Indeed, azides are connected to cells and hence rather immobile, whereas the DBCO moieties are connected to LNP which have diffusion coefficient which is several orders of magnitude [20] lower that e.g. the low molecular weight DBCO-$EG_4$-Fluor545 that performed so well in the initial conjugation experiments described earlier in this paper. Electrostatic interaction between LNP and the cell surface automatically increases the local DBCO concentration in the vicinity of the azide-labelled glycocalyx, thereby increasing the likeliness that both reaction partners react, which, in a broader sense, could be seen as a kind of proximity-driven ligation.

Flow cytometry analysis showed that a short 15 min co-incubation of LNP and cells was sufficient to achieve a massive extent of cell surface adsorption **(Figure 3)**, whereas in a parallel experiment performed at a pH of 7.4, only a very low degree of cellular fluorescence was measured. To alleviate the electrostatic interaction between the LNP and the cell surface, cells were subjected to triple washing with neutral buffer which led to a decrease in fluorescence of cells that were not metabolically azide labelled. By contrast, the cellular fluorescence of metabolically azide labelled cells incubated with DBCO LNP remained constant during repeated washing cycles with buffer at neutral pH. Taken together, these observations hint at a selective SPAAC conjugation of DBCO LNP to metabolically azide labelled cells. Tempering the enthusiasm on the use of this strategy, however, is the vast non-specific background adsorption of control LNP to control cells. Indeed, from the data in **Figure 3**, it is clear that despite multiple washing steps, control cells still exhibit a high fluorescence. To address this issue of high non-specific background binding, we reasoned that working at neutral pH is crucial to avoid electrostatic interaction between LNP and cells and to avoid the concomitant degree of irreversible association. We also reasoned that increasing the reactivity between the respective reaction partners on the LNP and cell surface could be of great benefit to improve upon the sluggish reaction between DBCO and azides under the present challenging conditions. To address these considerations, we explored the ultra-fast inverse electron demand Diels–Alder (IEDDA) reaction between tetrazines and trans-cyclooctene (TCO)[21][22], which is amongst the fastest bio-orthogonal reactions that can occur within a complex and diluted physiological environment. The simplest solution would be to metabolically label cells with either tetrazine or TCO in combination with LNP that bear the complimentary reaction partner. However, despite recent progress in the field, including the use of sialic acid derivatives [23] for which the metabolic machinery is more tolerant towards bulky substituents, metabolic glycocalyx labelling with more bulky unnatural motifs is still by far outperformed by azido sugars.

Hence, we opted to apply a 2-step conjugation sequence in which metabolically azide labelled cells are first reacted with sulfo-6-methyl-tetrazine-DBCO (DBCO-Tz), followed by co-incubation with TCO LNP. This route was fostered by our observation on SPAAC conjugation of DBCO-$EG_4$-Fluor545 **(Figure 1)** to metabolically azide labelled cells, proving that conjugation of low molecular weight compounds, in contrast to objects that are several orders of magnitude larger in size, can still be considered as very efficient. As a confirmation, we treated DBCO-Tz pulsed metabolically azide labelled cells with TCO-Cy5, followed by flow cytometry and confocal microscopy. **(Figure 4A)** From these data is clear that selective IEDDA occurs, with minimal cellular fluorescence the controls that lack metabolic azide labelling or that were not pulsed with DBCO-Tz. We then copied this experimental setting and pulsed metabolically azide labelled cells with DBCO-Tz followed by co-incubation with TCO LNP for 1 hour and analysis by flow cytometry and confocal microscopy. TCO LNP were assembled in a similar fashion as DBCO LNP by replacing DSPE-PEG-DBCO with DSPE-PEG-TCO. We also prepared TCO LNP with varying TCO density by dilution with DSG-PEG, **Table 1** lists the characteristics of these LNP too. **Figure 4** clearly demonstrates that the 2-step SPAAC/IEDDA conjugation strategy allows for a highly specific cell surface conjugation of LNP, with very low non-specific background fluorescence for controls cells lacking azides in their glycocalyx and when omitting the DBCO-Tz step. Furthermore, an increased density of TCO on the LNP surface affords a higher cellular association of LNP **(Figure 4C)**. The high density of LNP on the cell surface is further illustrated in **Figure S5** in the Supporting Information section which shows maximum intensity and 3D projections of LNP bound cells.

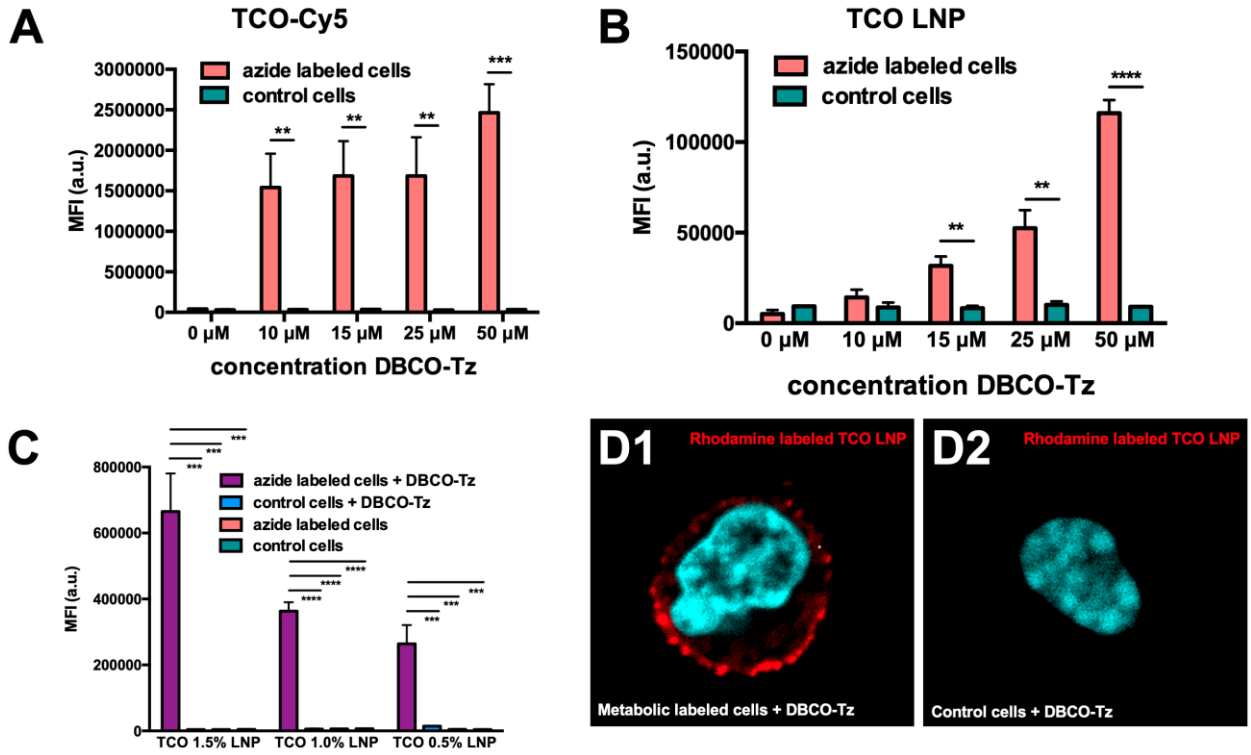


**Figure 4** | Flow cytometry analysis of metabolic labelled cells and control cells: (A) pre-treated with DBCO-Tz followed by incubation with TCO-Cy5, (B) pre-treated with DBCO-Tz followed by incubation with TCO LNP, (C) pre-treated or untreated with DBCO-Tz followed by incubation with TCO LNP 1.5%, 1.0% and 0.5%. n=3; t-test ** p<0,01; *** p<0,001; ****p<0,0001)(D) confocal microscopy of metabolic labelled cells (D1) and control cells (D2) pre-treated with DBCO-Tz followed by incubation with TCO LNP (red fluorescence). Cell nuclei were stained with Hoechst (cyan). Scale bar represents 5 micron.

## Conclusion

In conclusion, we have reported on a simple, yet efficient, methodology to covalently conjugate NP to the surface of living cells, using 2 consecutives click reactions. Whereas the SPAAC reaction between cell surface introduced azides (by virtue of metabolic labelling with azido sugars) and low molecular weight cycloalkynes is sufficiently fast to take place under common cell culture conditions, it was found to be sluggish to allow for conjugation of cycloalkynes-functionalized nanoparticles. By contrast, a two-step reaction, involving in a first step SPAAC reaction of cell surface azides with a low molecular weight cycloalkyne-tetrazine compound and in a second step reaction of cell surface tetrazines with transcycoalkene-functionalized NP by ultrafast IEDDA, allowed for highly specific covalent cell surface conjugation of NP. Importantly, this methodology lead to very low non-specific background binding of NP to cells, which was not be the case when relying on SPAAC only. We exemplify our case of lipid-based NP, but we believe it is generally applicable to a broad range of nanoparticles that can be functionalized on their surface with transcycoalkene moieties. Moreover, either the linkage between the transcycoalkene and the NP as well as the NP itself can be engineered in response to specific stimuli in the tumor microenvironment, topics which are under currently investigation in our labs. Shown here for the example of T cells, we envision the use of this methodology for adoptive cell therapy for multiple cell types and believe that and chemical conditioning (i.e. metabolic labelling) and conjugation steps are compatible with the common practice in the field.

## Acknowledgements

B.G.D.G. acknowledges funding from the European Research Council (ERC) under the European Union's Horizon 2020 research and innovation program (grant N° 817938) and funding from the FWO (grant N° G019819N).

**Keywords:** click chemistry • bioorthogonal • cell therapy • SPAAC • IEDDA

[1] M. T. Stephan, J. J. Moon, S. H. Um, A. Bershteyn, D. J. Irvine, *Nat. Med.* **2010**, *16*, 1035–1041.

[2] D. Li, X. Li, W. L. Zhou, Y. Huang, X. Liang, L. Jiang, X. Yang, J. Sun, Z. Li, W. D. Han, et al., *Signal Transduct. Target. Ther.* **2019**, *4*, DOI 10.1038/s41392-019-0070-9.

[3] P. Y. Li, Z. Fan, H. Cheng, *Bioconjug. Chem.* **2018**, *29*, 624–634.

[4] Y. Zheng, L. Tang, L. Mabardi, S. Kumari, D. J. Irvine, *ACS Nano* **2017**, *11*, 3089–3100.

[5] K. W. Yong, D. Yuen, M. Z. Chen, A. P. R. Johnston, *ACS Appl. Mater. Interfaces* **2020**, *12*, 5593–5600.

[6] R. P. Lyon, J. R. Setter, T. D. Bovee, S. O. Doronina, J. H. Hunter, M. E. Anderson, C. L. Balasubramanian, S. M. Duniho, C. I. Leiske, F. Li, et al., *Nat. Biotechnol.* **2014**, *32*, 1059–1062.

[7] A. Das, P. Theato, *Chem. Rev.* **2015**, DOI 10.1021/acs.chemrev.5b00291.

[8] M. T. Stephan, S. B. Stephan, P. Bak, J. Chen, D. J. Irvine,

*Biomaterials* **2012**, *33*, 5776–5787.

[9] Kenry, B. Liu, *Trends Chem.* **2019**, *1*, 763–778.

[10] N. J. Agard, J. A. Prescher, C. R. Bertozzi, *J. Am. Chem. Soc.* **2004**, *126*, 15046–15047.

[11] C. R. Prescher, Jennifer A. Bertozzi, *Nat. Chem. Biol.* **2005**, *1*, 13–21.

[12] A. Uvyn, R. De Coen, O. De Wever, K. Deswarte, B. N. Lambrecht, B. G. De Geest, *Chem. Commun.* **2019**, *55*, 10952–10955.

[13] H. Wang, R. Wang, K. Cai, H. He, Y. Liu, J. Yen, Z. Wang, M. Xu, Y. Sun, X. Zhou, et al., *Nat. Chem. Biol.* **2017**, *13*, 415–424.

[14] J. Zou, T. Kawai, T. Tsuchida, T. Kozaki, H. Tanaka, K. S. Shin, H. Kumar, S. Akira, *Immunity* **2013**, *38*, 717–728.

[15] E. C. Gale, G. A. Roth, A. A. A. Smith, M. Alcántara-Hernández, J. Idoyaga, E. A. Appel, *Adv. Ther.* **2020**, *3*, 2070001.

[16] J. K. Tom, E. Y. Dotsey, H. Y. Wong, L. Stutts, T. Moore, D. H. Davies, P. L. Felgner, A. P. Esser-Kahn, *ACS Cent. Sci.* **2015**, *1*, 439–448.

[17] Y. Chen, S. De Koker, B. G. De Geest, *Acc. Chem. Res.* **2020**, DOI 10.1021/acs.accounts.0c00260.

[18] S. Van Herck, K. Deswarte, L. Nuhn, Z. Zhong, J. P. Portela Catani, Y. Li, N. N. Sanders, S. Lienenklaus, S. De Koker, B. N. Lambrecht, et al., *J. Am. Chem. Soc.* **2018**, *140*, 14300–14307.

[19] K. H. Moss, P. Popova, S. R. Hadrup, K. Astakhova, M. Taskova, *Mol. Pharm.* **2019**, *16*, 2265–2277.

[20] D. Coglitore, S. P. Edwardson, P. Macko, E. A. Patterson, M. Whelan, *R. Soc. Open Sci.* **2017**, *4*, 1–9.

[21] Y. Takayama, K. Kusamori, M. Nishikawa, *Molecules* **2019**, *24*, DOI 10.3390/molecules24010172.

[22] R. D. Row, J. A. Prescher, *Acc. Chem. Res.* **2018**, *51*, 1073–1081.

[23] T. J. Sminia, H. Zuilhof, T. Wennekes, *Carbohydr. Res.* **2016**, *435*, 121–141.

## Entry for the Table of Contents

Insert graphic for Table of Contents here.

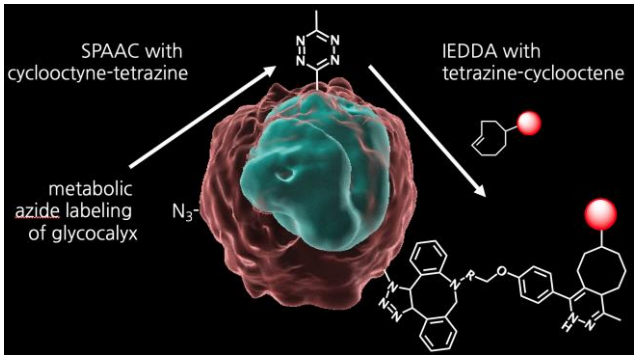


Live cells can be efficiently conjugated with nanoparticles on their surface by two successive biorthogonal click reactions.

Institute and/or researcher Twitter usernames: https://twitter.com/bruno_de_geest